Cytometry
PART A
Journal of the International Society for Advancement of Cytometry

A Novel Imaging-based High-throughput Screening Approach to Anti-angiogenic Drug Discovery

Lasse Evensen, David R. Micklem, Wolfgang Link, James B. Lorens*

Department of Biomedicine, University of Bergen, Bergen, Norway

Received 17 July 2009; Revision Received 21 August 2009; Accepted 14 September 2009

The authors thank Sisssel Vik Berge, Marianne Enger, and Paula Ruurs for excellent technical assistance.

Grant sponsor: Norwegian Research Council; Grant number: FUGE 183775; Grant sponsor: University of Bergen pre-doctoral and post-doctoral fellowships.

Address of David R. Micklem: BerGenBio A/S, Bergen, Norway.

Address of Wolfgang Link: Experimental Therapeutics Program, Centro Nacional de Investigaciones Oncologicas (CNIO), Melchor Fernandez Almagro 3, Madrid 28029, Spain.

*Correspondence to: James B. Lorens, Department of Biomedicine, University of Bergen, Jonas Lies Vei 91, N-5009 Bergen, Norway

Email: jim.lorens@biomed.uib.no

Published online 15 October 2009 in Wiley InterScience (www.interscience.wiley.com)

DOI: 10.1002/cyto.a.20808

Abstract

The successful progression to the clinic of angiogenesis inhibitors for cancer treatment has spurred interest in developing new classes of anti-angiogenic compounds. The resulting surge in available candidate therapeutics highlights the need for robust, high-throughput angiogenesis screening systems that adequately capture the complexity of new vessel formation while providing quantitative evaluation of the potency of these agents. Available *in vitro* angiogenesis assays are either cumbersome, impeding adaptation to high-throughput screening formats, or inadequately model the complex multistep process of new vessel formation. We therefore developed an organotypic endothelial-mural cell co-culture assay system that reflects several facets of angiogenesis while remaining compatible with high-throughput/high-content image screening. Co-culture of primary human endothelial cells (EC) and vascular smooth muscle cells (vSMC) results in assembly of a network of tubular endothelial structures enveloped with vascular basement membrane proteins, thus, comprising the three main components of blood vessels. Initially, EC are dependent on vSMC-derived VEGF and sensitive to clinical anti-angiogenic therapeutics. A subsequent phenotypic VEGF-switch renders EC networks resistant to anti-VEGF therapeutics, demarcating a mature vascular phenotype. Conversely, mature EC networks remain sensitive to vascular disrupting agents. Therefore, candidate anti-angiogenic compounds can be interrogated for their relative potency on immature and mature networks and classified as either vascular normalizing or vascular disrupting agents. Here, we demonstrate that the EC-vSMC co-culture assay represents a robust high-content imaging high-throughput screening system for identification of novel anti-angiogenic agents. A pilot high-throughput screening campaign was used to define informative imaging parameters and develop a follow-up dose-response scheme for hit characterization. High-throughput screening using the EC-vSMC co-culture assay establishes a new platform to screen for novel anti-angiogenic compounds for cancer therapy.

Key terms

high-throughput screening; endothelial/mural cell co-culture; angiogenesis

INHIBITING angiogenesis is a validated therapeutic modality for cancer (1). Hence, new agents that potently inhibit pathological angiogenesis are a critical component of future combination cancer therapies (2). The identification of candidate therapeutics relies on current *in vitro* angiogenesis assays that measure effects on endothelial cell migration, proliferation, apoptosis and tube formation, and *in vivo* models such as the chick chorioallantoic membrane assay, corneal neovascularization assay, and Matrigel plug assays (3–5). Current *in vitro* angiogenesis assays are generally focused on specific behaviors of monocultured endothelial cells (EC) (e.g., migration, proliferation) and fail to model heterotypic perivascular interactions, whereas *in vivo* systems are not compatible with high-throughput screening. More complex endothelial tube formation *in vitro* assays, such as endothelial culture on Matrigel or in 3D collagen matrices, are cumbersome and not sufficiently robust for high-throughput screening. To address this, we have developed a microtiter format *in vitro* assay that

ISAC
International Society for Advancement of Cytometry

encompasses the three main components of blood vessels: EC, mural cells, and the basement membrane. Co-culture of primary human umbilical cord endothelial cells (HUVEC) and pulmonary artery-derived vascular smooth muscle cells (PA-vSMC) results in formation of an organotypic capillary network recapitulating many facets of *in vivo* angiogenesis including morphology, pathfinding migration, loss of endothelial cell proliferation, basement membrane deposition, and quiescence. During network formation, EC are completely dependent on vSMC-derived VEGF. Inhibition of VEGF-signaling [by treatment with anti-VEGF antibody, (bevacizumab), VEGF receptor-targeting small molecule tyrosine kinase inhibitors, or RNA interference of VEGF expression in vSMC] potently blocks capillary-like network formation (6–9). However, once formed, EC networks acquire resistance to anti-VEGF therapeutics reflecting a phenotypic VEGF-switch characteristic of blood vessel maturation. This biphasic sensitivity profile can be utilized to classify potential anti-angiogenic therapeutics as normalizing agents (e.g. bevacizumab) or vascular disruptive agents (e.g. combretstatin) (8). Further, we have shown that image analysis of capillary-like network formation can be used to conduct quantitative structure-activity relationship analysis of tubulin-inhibitor natural compound derivatives (unpublished results). Here, we evaluate the biphasic co-culture assay as an automated high-throughput image-acquisition approach for anti-angiogenic compound discovery. Using a pilot HTS screening campaign, we evaluated image analysis parameters and assessed the robustness of the biphasic approach. We demonstrate that the HTS co-culture assay represents a novel organotypic assay approach suitable for large scale high-throughput screening.

Material and Methods

Compounds

PTK787/ZK (10) and CHIR258 (11) were kindly provided by Novartis (Oncology Research, Novartis Institutes for BioMedical Research). CK246 was kindly provided by Professor Karl-Heinz Altmann (Department of Chemistry and Applied Biosciences, Institute of Pharmaceutical Sciences, ETH Zurich, Zurich Switzerland) (12). Velcade was kindly provided by Prof. Bjørn Tore Gjertsen, Haukeland University Hospital, Norway (13). Flavopiridol was kindly provided by the NCI, National Institutes of Health. All other chemicals were purchased from commercial sources. 5-Aza-2'-Deoxycytidine, Bapta-AM, Doxorubicin, JAK3 Inhibitor VI, JNK Inhibitor VIII, Kenpaullone, KN-62, Resveratrol, W-13 HCl, and W-7 HCL were purchased from Calbiochem (San Diego, CA). Genistein, Rapamycin, Thapsigargin (THAPS), and U0126 were purchased from LC Laboratories. (Woburn, MA,); Caffeine, Hydrocortisone, Nicotinamid, Paclitaxel, STO-609, 12-O-tetradecanoylphorbol-13-acetate (TPA), Trichostatin A (TSA), and Vinblastine were purchased from Sigma–Aldrich (St. Louis). D000 was purchased from Labotest (Niederschoena, Germany); Stock solutions of the test compounds were deposited onto 96-well mother plates, transferred to multiple replica plates, and frozen at −80°C.

Cell Culture

HUVEC and PA-vSMC were purchased from Lonza (C2517A, CC2581). To simplify imaging, early passage HUVEC cells were infected with retrovirus carrying a fluorescent-expressing construct. HUVEC cells used in screening experiments were infected with a dsTomato construct, whereas a GFP construct was used for the experiments testing the use of propidium iodide staining. Cells were maintained in culture in the supplier's recommended complete medium (EGM-2, SmGM-2) at 37°C, 5% CO_2. The growth medium was changed every third day, and cells were passaged before reaching confluence. The maximum passage number used for experiments was eight (HUVEC) and 10 (PA-vSMC).

EC-mural Cell Co-culture Assay

Separated cultures of PA-vSMC and HUVEC were trypsinated, counted and mixed in a falcon-tube, and centrifuged at 200*g* for 5 min. To seed the co-cultures, the cell pellet was resuspended in the desired amount of EGM-2 before distributing to the wells of a 96-well plate. The plate was then centrifuged briefly at 200*g* to achieve an even distribution of cells and cultured for 72 h at 37°C, 5% CO_2 to allow network formation. Cell numbers and culture volume were as follows (per well): 96-well plates: 5×10^4 PA-vSMC, $10–15 \times 10^3$ HUVEC, 200 μl EGM-2.

Compound Treatment

Addition of compounds was performed as follows: Concentrated stock solutions were diluted to 2× concentrations in a 96-well plate containing 100 μl EGM-2 per well and mixed thoroughly; 100 μl medium was removed from seeded co-cultures and substituted with 100 μl EGM-2 containing 2× compound concentrations. DMSO concentrations were kept at 0.25 %.

Microscopy and High-content Imaging

For quantitative analysis of the co-cultures, a BD Pathway 855 bioimaging system (BD Biosciences, San Jose, CA) was used for automated high-throughput-imaging. Statistical analysis of acquired images was done with BD Image Data Explorer software. Images demonstrating network formation were acquired as 5 × 5 montages with a 10× objective (Fig. 1). To decrease disk usage and acquisition times, images from screening experiments and dose-response experiments were acquired as 2 × 2 montages using a 10× objective. Filters used: Propidium Iodide: excitation filter 555/28 and emission filter 645/75, Hoechst: excitation filter 380/10 and emission filter 435LP, dsTomato HUVEC cells: excitation filter 548/20 and emission filter 570LP, GFP HUVEC cells: excitation filter 488/10 and emission filter 520/35. Background subtraction, noise reduction (rolling ball 25 × 25), and image thresholding were performed using the AttoVision v1.6.1 software supplied by BD Biosciences. Statistics on tube branch lengths per region of interest were obtained using the "Tube Formation" image analysis module of AttoVision v1.6.1.

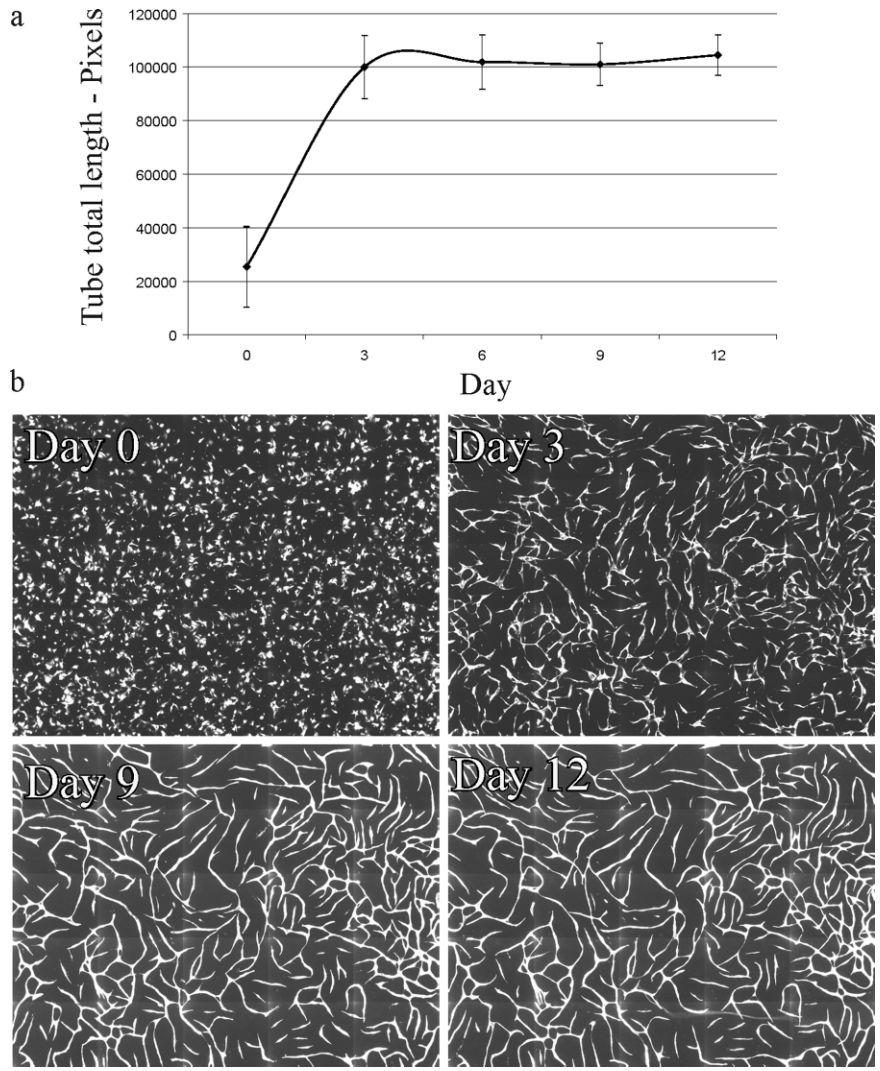

Figure 1. Parameter evaluation. (**a**) Twelve EC-vSMC co-cultures were seeded in a 96-well plate and networks were allowed to develop without any interference. Images were acquired for every third day as 5× 5 montages with a ×10 objective and quantified with the parameter tube total length (BD Attovision software). Once the network is formed at day 3, this parameter reflects the stability of the network (day 3—12), and inhibition of network formation due to drug treatment can be measured. (**b**) Images from a developing network acquired every third day during a 12-day period showing fluorescent EC (gray). Individual seeded EC (day 0), the EC gradually interact to generate a capillary-like network (day 3). The generated network is remodeled and matures over time as the branches become more even and defined (day 9). The final network is stable and can be kept alive over long periods of time (Day 12). vSMC are not visible in the images but generate a confluent layer beneath the fluorescent EC.

dsTomato/GFP-Expression

Expression of proteins in cells was performed by transfection of a 293 T packaging cell line with a retroviral expression vector containing the DNA of interest (14). Virus was harvested 24–48 h after transfection in medium suited for the target cells. Infection was performed by filtering the virus containing medium, addition of protamine sulfate, and transferring of the virus containing medium to the target cells that were incubated further for 24 h. Infection was ended by changing the medium. Protocol will be given out by request. GFP was expressed from pCGFP (15). tdTomato was expressed from pCtdTomato, a derivative of pCGFP with the GFP replaced by tdTomato (16).

Hoechst and Propidium Iodide Staining

Co-cultures were stained with 1 μg/ml Propidium Iodide (dead cells) and/or 10 μg/ml Hoechst 33,342 (nuclei) in EGM-2 for 30 min at 37°C, 5% CO_2, and imaged as described. To avoid difficulties with separating propidium iodide fluorescence from tdTomato fluorescence, these experiments were conducted with GFP-expressing HUVEC cells.

IC_{50} Calculations

IC_{50} values were calculated from a nine-point dose-response curve drawn from two replicates using the log[inhibitor] versus response function in Prism Graphpad 5.

Statistics

Nine DMSO-treated co-cultures were included on each of the replicate plates. Threshold values corresponding to three standard deviations were calculated based on the mean tube total length from these DMSO-controls. In the screen, wells producing tube total length values outside the threshold values were defined as a hit. In order for a compound to be included in follow-up dose-response experiments two out of three replicates had to be scored as a hit.

Standardization

Values from replicate plates with treated co-cultures were standardized for direct comparison in the same plot using the formula:

$$\frac{(\text{Tube total length single well} - \text{Mean whole plate})}{\text{St Dev Whole plate}}$$

Z-factor Calculation

A 96-well plate containing 84 DMSO-treated (0.25 %) and 12 CHIR258 (30 nM) co-cultures was incubated for 3 days and imaged as 2 × 2 montages. Average total tube lengths and standard deviations were quantified for the two treatment groups, and noise/signal ratio calculations were performed using the formula:

$$1 - \frac{(3\times(\text{SD}_{\text{NegCtrls}} + \text{SD}_{\text{PosCtrls}}))}{\text{Avg}_{\text{NegCtrls}} - \text{Avg}_{\text{posCtrls}}}$$

Results

Measuring Cellular Networks

The co-culture assay entails live image analysis of fluorescent protein-expressing primary human EC that form tubular networks within 72 h postseeding (6). Unless otherwise specified, the EC used in this study were transduced with a tdTomato retroviral expression construct to ensure stable expression of the fluorescent marker.

The EC networks form over a period of 3 days. At day 0 and day 1, the EC are elongated and display extensive migratory activity (data not shown). As they begin to integrate into a proper network (Day 3, Fig. 1b), the EC interdigitate to generate tubes with uniform diameter (6). The EC do not proliferate when co-cultured with vSMC, so the networks do not grow in size. However, the connectivity increases until the network stabilizes, and once formed, the network can be kept alive for long periods (Figs. 1a and 1b). Although early networks are susceptible to anti-VEGF therapeutics, stable networks become resistant to anti-VEGF therapeutics (Evensen et al., submitted).

Ideally, the parameters used to quantify EC networks should reflect the stability of a generated network and also be able to identify any inhibited phenotype. To investigate the stability of the parameters available in the BD Attovision v1.6.1 software, 12 untreated co-cultures were seeded in a 96-well plate and monitored over a period of 12 days. The most stable imaging parameter was found to be tube total length (Fig. 1a), which estimates the total length of cellular tubes within the field of view. Developed networks, with their extensive interconnections, have longer total tube lengths than inhibited phenotypes (Figs. 2c, 2f, and 2g).

The tube total length parameter is calculated on the basis of a segmentation mask-defined preanalysis that divides the image into regions that are part of the cellular network and regions that are considered to be background (Figs. 2b and 2e). The segmentation mask can be used to define both the tube bodies (Figs 2b and 2e) and to generate a one-pixel-wide skeleton representation of the network structure (Figs. 2c and 2f). The tube total length parameter corresponds to the total number of pixels in this skeletonised image. To optimize images during analysis, noise was reduced by background subtraction and a 25× 25 pixel sized rolling ball filter. A further size-based filter was included to exclude any objects under 8000 pixels in size from the analysis.

The Z-factor for tube total length was calculated from 84 individual DMSO treated co-cultures (negative control) and 12 co-cultures treated with the VEGFR2 tyrosine kinase inhibitor CHIR258 (positive control) in a 96-well plate and imaged as 2× 2 montages with a 10× objective at day 3 (Fig. 2). CHIR258 generates rounded-up, single viable EC morphology phenotype representative of nontoxic anti-angiogenic compounds (Fig. 2d) (11). Following image analysis and quantification of tube total length, a Z-factor of 0.68 was calculated, indicating that the co-culture assay is highly suitable for large-scale HTS campaigns.

Identification of Screening Hits

Two small molecule tyrosine kinase inhibitors PTK787/ZK and CHIR258 were used as model anti-angiogenic compounds to demonstrate hit identification. PTK787/ZK and CHIR258 inhibit autophosphorylation of VEGFR-2 and both were used to show that compounds with similar targets give similar phenotypes (10). Based on four DMSO (vehicle control) treated replicates, the average and standard deviation of the tube total length was calculated (Fig. 3a, blue line). Quantification of PTK787/ZK (100 nM) and CHIR258 (100 nM) treated co-cultures showed consistent inhibition to levels greater than three standard deviations from the DMSO controls (Fig. 3a, red line), delineating the inhibited phenotype (Fig. 3b, lower panel). Hits for the co-culture imaged-based high-throughput screen were thus defined as wells producing tube total length values exceeding three standard deviations from the mean of the DMSO control.

Compounds that have a nonspecific cytotoxic effect could be a significant source of false positives in a high-throughput screen. We demonstrated (Fig. 3c) that a simple viability marker such as propidium iodide (which is only able to enter cells with a disrupted plasma membrane) could be used to identify co-cultures with extensive cytotoxicity and exclude them from follow-up dose-response experiments. Both proteosomal inhibition by bortezimid (Velcade) at 200nM and anti-VEGF treatment with PTK787/ZK (100 nM) result in inhibition of network formation. However, the Velcade causes

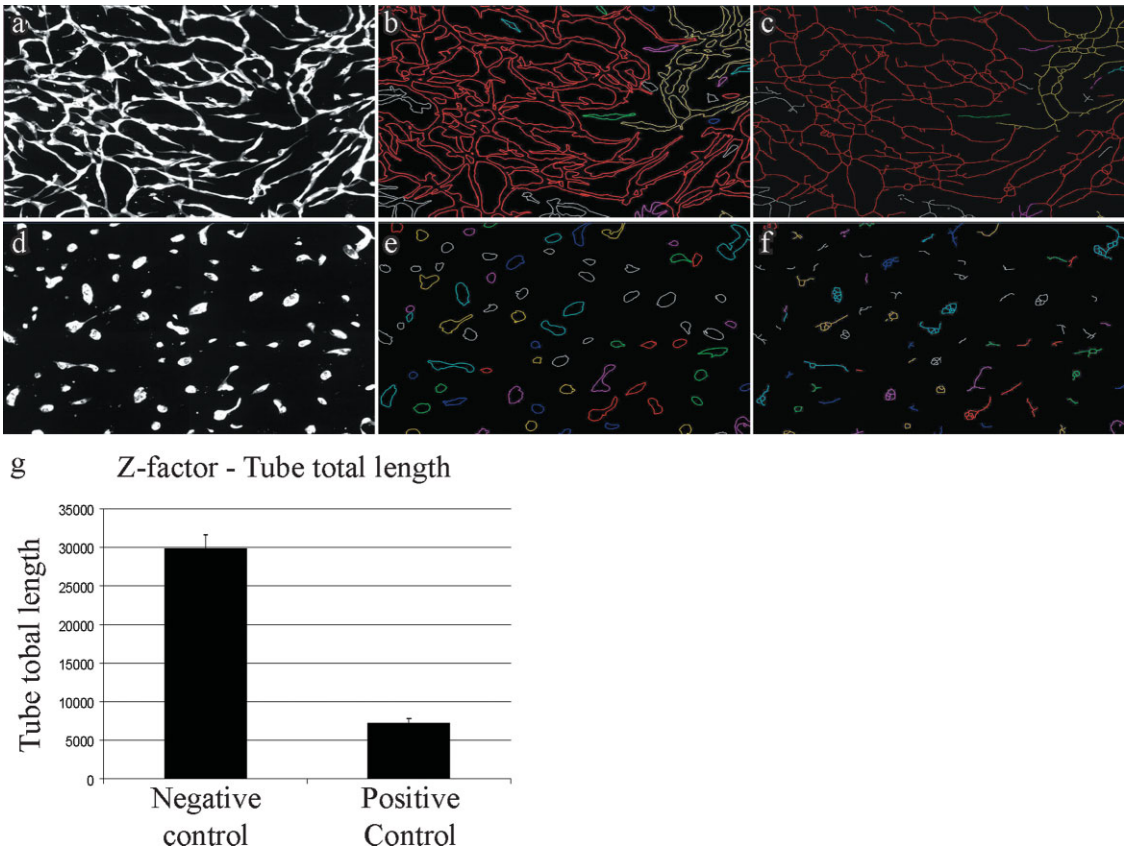

Figure 2. Image segmentation and quantification. For Z-factor calculation, 84 DMSO (0.25 %) and 12 CHIR258 (30 nM) treated co-cultures were seeded in a 96-well plate. Panel **a—c** represents the DMSO treated co-cultures (negative control) and panel d-f represents the CHIR258 treated co-cultures (positive control). (a, **d**) 2× 2 montage images (×10 objective) of fluorescent EC (gray) in co-culture with vSMC were acquired at day 3. (b, **e**) Fluorescent cells are recognized by thresholding and rolling ball filtering (RB 25× 25) to produce a binary segmentation mask. Analysis of the segmentation mask produces an outline of the tube bodies with unconnected segments given a unique color. (c, **f**) Skeletonization of the segmentation mask produces a one pixel-wide representation of the EC structures with the skeleton located along the centres of the tube body structures. The skeletonised version of the EC structures are measured in pixels and developed networks (c) score higher because they have larger tube total length values than inhibited phenotypes (f). (**g**) The Z-factor is 0.68 for the parameter tube total length, (see Material and Methods) and positive controls (known inhibitors of network formation) have significantly shorter tube total lengths than negative controls. [Color figure can be viewed in the online issue, which is available at www.interscience.wiley.com.]

significant PI uptake indicating that it has cytotoxic effects. In contrast, the inhibitory effect of PTK787/ZK is not due to cytotoxicity. Because PI-staining overlaps with tdTomato (RFP) emission, these experiments were performed in combination with GFP-expressing EC.

Proof of Principle: High-throughput Screening

To evaluate consistency in screening hit identification, a double-blinded pilot screen was conducted using a prearrayed compound plate comprising randomly distributed small molecule VEGFR2 tyrosine kinase inhibitors, PTK787/ZK (200 nM and 50 nM) and CHIR258 (200 nM and 50 nM), and two vascular disruptive agents, combretastatin CA-4 (100 nM and 20 nM) (17–19), an inhibitor of microtubule polymerization, and CK246 (100 nM and 20 nM), an epothilone analog functioning as a microtubule stabilizer (12), among DMSO control wells. Two 96-well plates seeded with EC-vSMC co-cultures were treated with the compound plate that also contained nine DMSO controls for calculation of a threshold value (Fig. 4a, red lines). After a 72 h incubation, the two screening plates were analyzed to identify active compounds. Plate 1 identified 26 wells and plate 2 identified 28 wells with tube total lengths below the threshold value. Unblinding the compound plate layout showed that 29 wells contained an active compound corresponding to a correct hit identification of over 90%; one false positive well was identified (0.05%) (Fig. 4b). Standardization of the data for direct comparison of the two plates show that the negative value distrubutions overlap, indicating that the co-culture assay consistently identifies inhibited phenotypes (Fig. 4c). Images from treated co-cultures show severely inhibited phenotypes that is clearly distinguishable from developing networks (Fig. 4d)

High-throughput Screening of a Small Molecule Compound Library

A blinded image-based co-culture HTS screen was performed using a subcollection of commercially available small

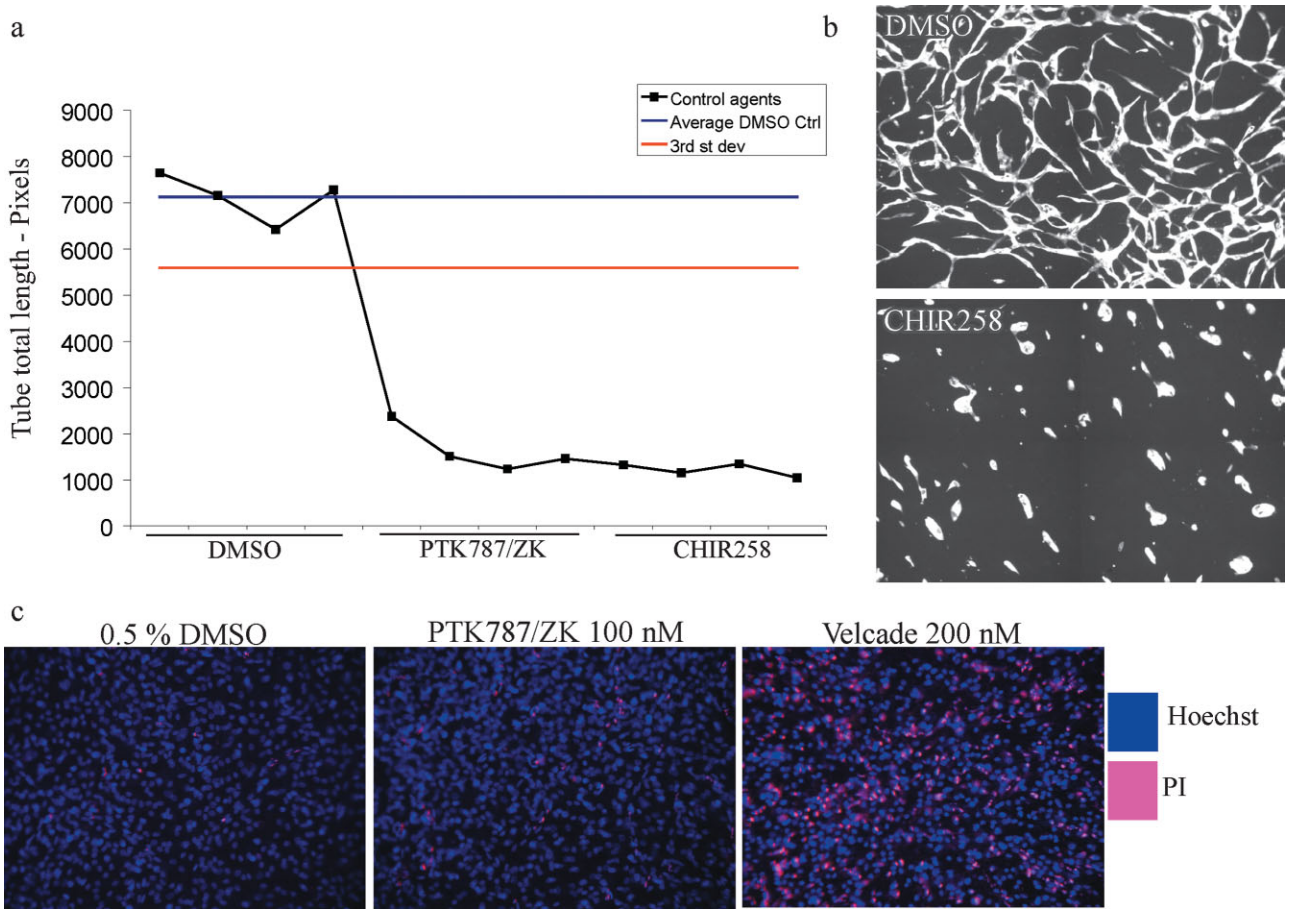

Figure 3. Identification of screening hits. (**a**) Co-cultures treated with 0.25% DMSO, 100 nM PTK787/ZK and 100 nM CHIR258 were imaged as 2× 2 montages at day 3 postseeding with a ×10 objective and quantified. Average tube total length for the four DMSO treated co-cultures (blue line) was the basis for calculation of the threshold value of three standard deviations away from the mean of DMSO treatment (red line). Both anti-VEGF therapeutics produced tube total length values exceeding three standard deviations from the mean of the DMSO control and would therefore be considered as hits. (**b**) A vehicle treated co-culture results in a developing network (upper panel, day 3), whereas anti-VEGF therapeutics inhibits network formation and results in a classical rounded-up, single cell morphology (Day 3, lower panel). (**c**) As a demonstration of identification of toxic compound effects co-cultures with GFP-expressing EC were stained with Hoechst and propidioum iodide (PI). Significant PI staining is observable with proteasome inhibitor Velcade treatment at high doses (200 nM), illustrating the staining profile of toxic compounds. [Color figure can be viewed in the online issue, which is available at www.interscience.wiley.com.]

molecule compounds previously used for chemical genetic studies (20). Compound screening plates comprised prearrayed DMSO-dissolved agents that were added directly to seeded co-cultures. Both the identity and location of the active agents versus multiple DMSO vehicles were blinded. Three identical co-culture HTS assays were conducted such that each compound screening plate well was assayed in triplicate. After incubation for 72 h to allow EC network formation, wells were imaged automatically as 2 × 2 montages with a 10× objective and tube total length was quantified for each image (Fig. 5a). At least two of three replicates had to show effects on tube total length greater than three standard deviations from the mean control wells to qualify as a primary screening hit. Figure 5b shows the overlaid standardized screening data from all three plates to illustrate the consistency of the assay screening hits. Overall, the replicates showed very good consistency with the identical 27 wells being indentified as screening hits in each assay plate.

Dose-response Experiments with Screening Hits

The primary pilot screening campaign was performed double-blinded and revealing compound identity showed the most potent agents comprised three major classes. The three compound classes included the microtubule-interfering agents vinblastine and paclitaxol, the histone deacetylase- (HDAC) inhibitor trichostatin A (TSA), and finally the Ca^{2+}-homeostasis interfering agent THAPS. Two other agents associated with Ca^{2+}-signaling, BAPTA and W13, were included to further investigate the importance of this process as they have opposite effects to THAPS. Thus, in total six compounds were further investigated in dose-response experiments to confirm their activity.

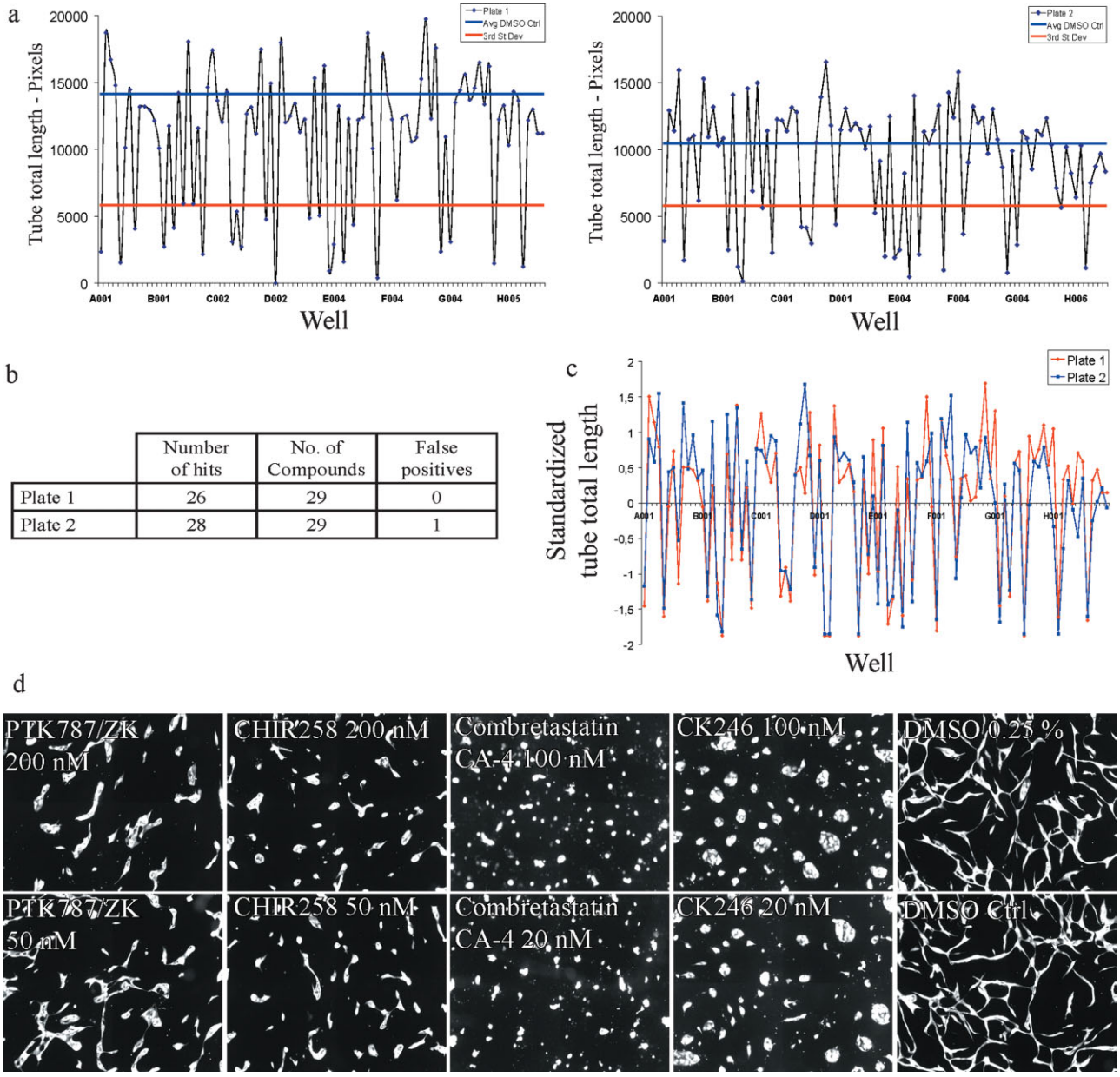

	Number of hits	No. of Compounds	False positives
Plate 1	26	29	0
Plate 2	28	29	1

Figure 4. Proof-of-concept: High-throughput screening. Four compounds, two anti-VEGF therapeutics and two vascular disruptive agents were distributed (double-blind) on a 96-well compound plate and two replicate plates with freshly seeded co-cultures were treated with nontoxic concentrations. (**a**) Nine co-cultures known to be treated with 0.25% DMSO were the basis for calculation of the threshold value of three standard deviations away from the DMSO-mean (red line). (a, **b**) Plate 1 and plate 2 identified 26 and 28 wells producing tube total lengths below the threshold value, respectively. On the two replicate plates only one false positive was produced. (**c**) Standardization of the screening data for direct comparison show overlapping results in the negative area emphasizing the consistency in hit identification. (**d**) The inhibited phenotypes produced by the individual compounds are easily distinguished from the developing DMSO-treated networks and score as significantly shorter networks when measured by the parameter tube total length. [Color figure can be viewed in the online issue, which is available at www.interscience.wiley.com.]

Microtubule-inhibitor compounds: Vinblastine and paclitaxel. Vinblastine, a member of the vinca alkaloids compound class, is an antimitotic drug with high affinity for tubulin (21). Upon binding tubulin, vinblastine inhibits microtubule formation, thereby arresting cells in the M phase of the cell cycle and inhibiting cell division. Vinblastine blocks formation of the endothelial tubes at picomolar concentrations and is a potent anti-angiogenic agent in the *in vivo* chick embryo chorioallantoic membrane (CAM) assay (22). Congruent with this, we observe a dose-dependent inhibition of capillary-like network formation (IC50 = 0.26 nM) in the EC-vSMC co-culture assay (Fig. 6a). Vinblastine-treated co-cultures yield cultures with rounded, unconnected, unicellular EC. Paclitaxel, a taxane, binds and stabilizes microtubule

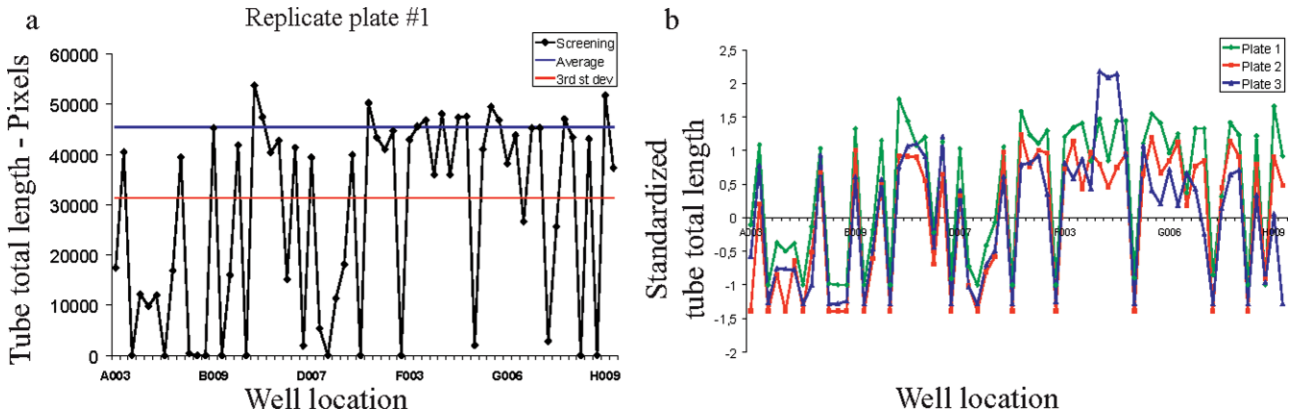

Figure 5. High-throughput screening of a small molecule compound library. A pilot image-based high-throughput screening using the *in vitro* EC-vSMC co-culture assay was performed blindly with a subcollection of commercial available small molecule compounds. (**a**) Tube total lengths were quantified for each well and the profile for one of three replicate plates is shown. Several wells produce tube total lengths outside the area of three standard deviations away from the DMSO-mean. (**b**) Overlaid standardized screening data from the three replicate plates illustrate the consistency of the hit identification as the curves overlap in the negative area. [Color figure can be viewed in the online issue, which is available at www.interscience.wiley.com.]

bundles (23). Paclitaxel exhibits similar inhibitory effects (IC50 = 1.3 nM) on network formation as vinblastine (Fig. 6b).

HDAC inhibitor TSA. The HDAC-inhibitor TSA blocks class I and II HDACs leading to alterations in chromatin structure that modulate gene expression (24). TSA has been shown to inhibit hypoxia- and VEGF induced angiogenesis (25–27). *In vivo*, it is a potent inhibitor of angiogenesis as it reduces neo-vessel formation in the CAM-assay and inhibits bFGF-induced angiogenesis in the Matrigel-plug assay in mice. In the primary screen performed with the EC-vSMC co-culture, TSA supported the inhibiting effects reported, although at very high concentrations (20 μM). Dose-response experiments showed that the IC50 value was 1.5 μM and maximum blocking effect was first observed at 5 μM (Fig. 6c).

Ca^{2+}-homeostasis interfering agents. Ca^{2+}-homeostasis interfering agents were identified in the primary screen. THAPS is an inhibitor of the Ca^{2+}-dependent ATPase pump that concentrates calcium in the sarcoplasmic and endoplasmic reticulum. By blocking this ATPase pump, THAPS treatment raises cytosolic Ca^{2+} concentrations (28). In the EC-vSMC co-culture assay, THAPS in the concentration range tested showed an inhibitory effect (IC50 5.7 μM, Fig. 6e). In contrast, BAPTA, a Ca^{2+}-chelator, only showed inhibitory effects above 10 μM suggesting that depleting Ca^{2+} in the medium does not have a substantial effect at subtoxic concentrations (Fig. 6f). Cytoplasmic Ca^{2+} is sequestered by Ca^{2+}-binding proteins, including calmodulin, that alter conformation and interact with specific target proteins, such as Ca^{2+}/calmodulin-dependent protein kinases (29). The calmodulin inhibitor W13 did not affect network formation indicating that calmodulin-dependent signaling is not required for endothelial network formation (Fig. 6d).

Together, these results confirm the inhibitory effects of vinblastine, paclitaxel, TSA, and THAPS found in the primary pilot high-throughput screening campaign. This demonstrates that the EC-vSMC *in vitro* angiogenesis co-culture assay is a reliable high-throughput screening platform to screen for novel anti-angiogenic agents.

DISCUSSION

Image Analysis Parameters for a High-throughput Screen

The live cell imaging-based high-throughput screening approach using the EC-vSMC co-culture assay robustly generates automated universal format (TIFF) images of endothelial cellular networks suitable for processing by any image analysis software. To obtain reliable, quantitative data, a primary imaging parameter must be used that accurately reflects the temporal acquisition of a stable endothelial network (8). We evaluated several imaging algorithms available in the Attovision v1.6.1 software package (Becton-Dickinson) that were designed to measure features of a branching network. The most reliable parameter was tube total length (field summary), which quantifies (in pixels) the total length of all tubes in the image field. This parameter is suitable as inhibited or disrupted networks comprise unconnected, rounded-up EC and thus, will score as "shorter" than fully developed networks (Fig. 2). Several other parameters were evaluated including tube average length, number of branch points, and tube max length. However, although the number of branch points is a highly suitable parameter to quantify networks, it did not reflect true endothelial network branch points. Figure 2 illustrates two stages in the image analysis: initial thresholding produces a segmented image where the fluorescent protein-expressing EC are distinguished from the background. The segmented image is then trimmed to a single pixel wide skeleton that represents all of the branches of the

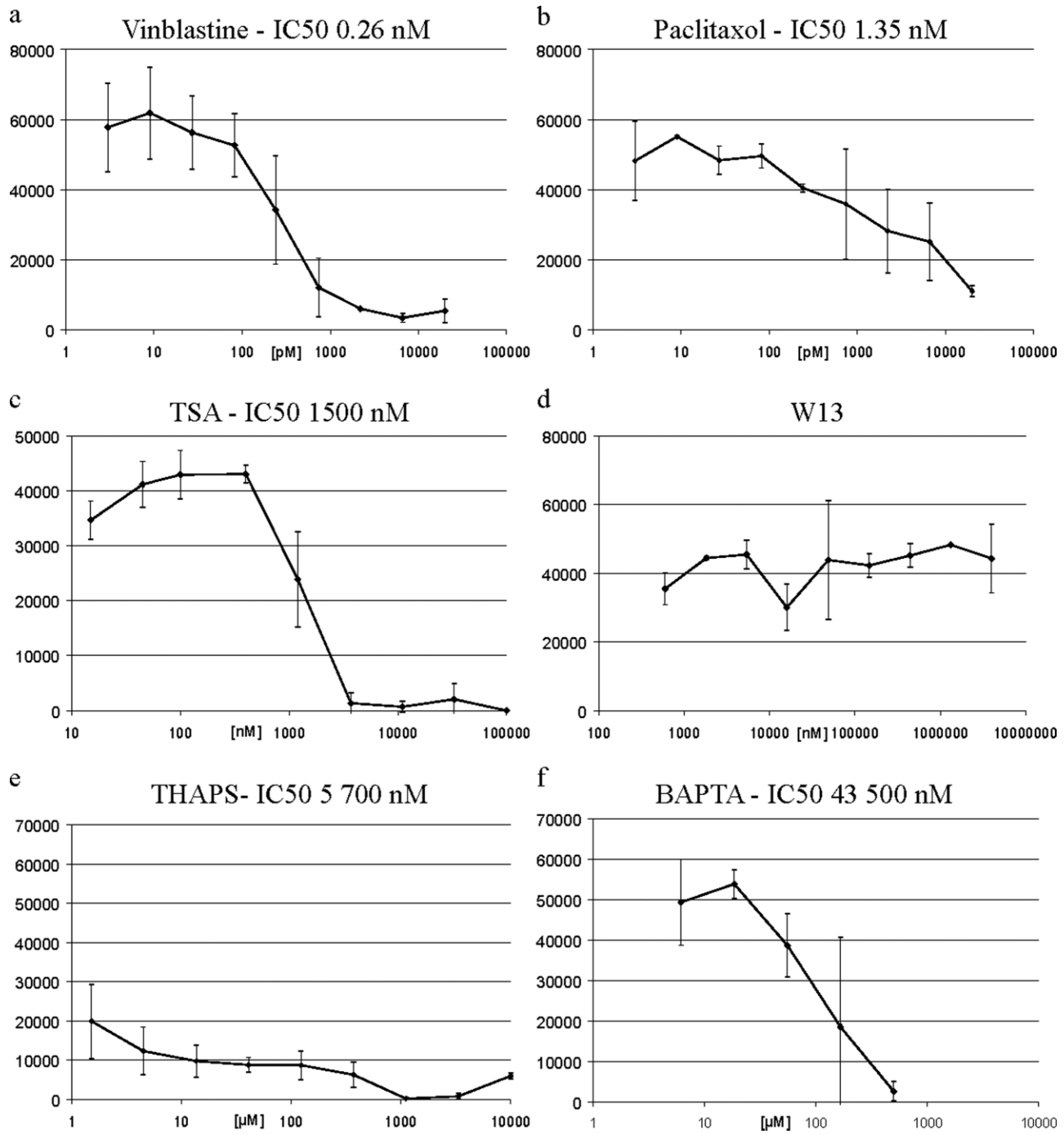

Figure 6. Dose-response experiments with identified hits. Six compounds were followed up in dose-response experiments based on the hits in the screen. (**a**) Vinblastine and paclitaxol are well known vascular disruptive agents and display very potent dose-dependent inhibitory effects in the nanomolar range verifying their anti-angiogenic effect in this assay. (**b**) The HDAC-inhibitor TSA was tolerated up to 1 μM but higher doses showed a sharp inhibitory effect. (**c**) The initial screen identified three Ca^{2+}-homoeostasis regulating compounds: THAPS, a compound that leads to raised cytoplasmic Ca^{2+}, showed strong inhibitory effects at all doses tested whereas BAPTA, a Ca^{2+}-chelating agent had little effect except at very high doses. W13, a calmodulin inhibitor, did not exert any effect on network formation.

network. As shown in 2c, the algorithm used in the Attovision software package produces spurious circular structures within the skeletonized network that interfere with calculation of the correct number of branch points.

The Z-factor for the parameter tube total length is 0.68 and thus, meets the standards for high-throughput screening (30). The value of the Z-factor is dependent on the number of EC seeded in each well. For calculation of the Z-factor, 15,000

EC/well were used which ensure a dense network and lower variation in tube total length between individual wells. The screening data obtained with 10,000 EC/well gave lower network density and a Z-factor at 0.2 (data not shown). Ideally the Z-factor should be >0.5; however, considering the differences between inhibited co-cultures and uninhibited co-cultures with developing tubes, the two extreme phenotypes are clearly distinguishable. By visual inspection, all inhibited phenotypes can easily be identified, and Figures 3 and 4 clearly demonstrate that hits are reliably identified by computer software. This is further emphasized by the low level of false positives (one false positive were scored as a hit) in the proof of principle screen (Fig. 4b). In both screens performed in this study, the overall similarity between the graphs of standardized data (Figs. 4b and 5b) emphasizes how consistently the tube total length parameter identifies inhibited phenotypes. Nevertheless, future screens will be performed with the conditions giving the best z-score value.

Dose-response Experiments

Previous findings demonstrate that EC in co-culture with vSMC do not proliferate (8,31). It is therefore somewhat unexpected that vinblastine and paclitaxel have such potent inhibitory effects as they are primarily used as antimitotic drugs in cancer treatment. However, their modes of action might explain their strong inhibitory effect: vinblastine inhibits microtubule assembly by binding to tubulin subunits, whereas paclitaxel hyperstabilizes the structure of microtubules and prevents them from disintegration (23,32). As a result both drugs, in addition to being anti-proliferative, affect cell motility and morphological changes that are dependent on microtubule dynamics (33). Hence, the inhibitory effect on network formation is likely due to impaired elongation and migration characteristic of pathfinding EC during angiogenesis. Our findings confirm the reported anti-angiogenic effects of vinblastine and paclitaxel observed in other *in vitro* and *in vivo* angiogenesis assays (22,34).

TSA is a selective inhibitor of histone deacetylase classes I and II but not class III. TSA alters gene expression by inhibiting the removal of acetyl groups from histones, hence changing the ability of DNA transcription factors to interact with DNA and altering DNA transcription (24). Gene transcription profiles have been shown to change in both EC and vSMC when co-cultured (35). Thus, identification of this compound in the primary screen likely reflects alteration of the EC gene expression changes requisite for network formation, albeit only at relatively high concentrations. In addition, it has been shown that TSA reduces hypoxia-induced migration and adherence of bovine aortic endothelial cells to diverse extracellular matrix proteins, among them collagen Type IV and fibronectin (26). Therefore, TSA might also modulate the interaction between EC and basement membrane proteins (e.g. collagen IV, XVIII, fibronectin), (8) deposited during network formation and inhibit haptotactic endothelial cell migration (Fig. 6c).

Ca^{2+}-homeostasis is important for numerous EC functions including proliferation, invasion, and differentiation (36), and perturbations of the fine-tuning of Ca^{2+}-levels results in altered cell signaling. For example, THAPS potently inhibited angiogenesis in the rat aorta assay in a dose-dependent manner via inhibition of proliferation and migration of EC (28). THAPS identified in the primary screen, as shown in the dose-response experiments, exhibits effects at the lowest dose tested (1.5 μM) and ideally, it should be tested in much lower concentrations. In fact, it has been shown that doses lower than 10 nM were able to potently inhibit migration and proliferation of vSMC *in vitro* monocultures (37,38), suggesting that the observed effects on EC networks could be attributed to effects on vSMC functions. Nevertheless, the result shows that increasing calcium in the cytosol efficiently inhibits network formation. The opposite effect, Ca^{2+}-depletion, was also tested by addition of BAPTA that chelates exogenous Ca^{2+}. However, an IC50 value at 45 μM indicates that Ca^{2+} in the medium is not important for network formation. The calmodulin inhibitor W13 also did not have any effect on network formation. Together, these results suggest that intracellular Ca^{2+}-levels must be kept below a threshold level to maintain the ability of network formation.

In conclusion, we show here that the organotypic endothelial-mural co-culture capillary-like network approach represents a robust new platform for live cell high-content imaging high-throughput screening for novel anti-angiogenic agents. Via a pilot HTS small molecule compound screening campaign, we demonstrate that informative imaging parameters facilitate the identification of known and novel angiogenic modulators. The screening system interrogates endothelial network formation in a native context comprising the three main components of blood vessels: EC, mural cells, and the basement membrane deposited as a result of the heterotypic cell-cell interaction. The screening system affords the opportunity to conduct HTS campaign on networks modeling both immature and mature vasculature.

Acknowledgments

The authors thank Sisssel Vik Berge, Marianne Enger, and Paula Ruurs for excellent technical assistance.

Literature Cited

1. Hurwitz H, Fehrenbacher L, Novotny W, Cartwright T, Hainsworth J, Heim W, Berlin J, Baron A, Griffing S, Holmgren E, Ferrara N, Fyfe G, Rogers B, Ross R, Kabbinavar F. Bevacizumab plus irinotecan, fluorouracil, and leucovorin for metastatic colorectal cancer. N Engl J Med 2004;350:2335–2342.
2. Jain RK. Normalizing tumor vasculature with anti-angiogenic therapy: A new paradigm for combination therapy. Nat Med 2001;7:987–989.
3. Auerbach R, Lewis R, Shinners B, Kubai L, Akhtar N. Angiogenesis assays: A critical overview. Clin Chem 2003;49:32–40.
4. Tran TC, Sneed B, Haider J, Blavo D, White A, Aiyejorun T, Baranowski TC, Rubinstein AL, Doan TN, Dingledine R, Sandberg EM. Automated, quantitative screening assay for antiangiogenic compounds using transgenic zebrafish. Cancer Res 2007;67:11386–11392.
5. Norrby K. In vivo models of angiogenesis. J Cell Mol Med 2006;10:588–612.
6. Evensen L, Micklem DR, Blois A, Berge SV, Aarsaether N, Littlewood-Evans A, Wood J, Lorens JB. Mural cell associated VEGF is required for organotypic vessel formation. PLoS One 2009;4:e5798.
7. Evensen L, Micklem DR, Blois A, Littlewood-Evans A, Wood J, Lorens JB. Mural cell associated VEGF is required for organotypic vessel formation. PlosOne 2009; vol 4 (6).
8. Evensen L, Micklem DR, Blois A, Vik-Berge S, Aarsæther N, Littlewood-Evans A, Wood J, Lorens JB. Mural cells regulate temporal endothelial VEGF-dependency and therapeutic resistance. In press.

9. Evensen L, Micklem DR, Blois A, Littlewood-Evans A, Wood J, Altmann KH, Odlo K, Hansen TV, Lorens JB. A biphasic profiling approach to discriminate normalizing and vascular disrupting agents. In press.
10. Wood JM, Bold G, Buchdunger E, Cozens R, Ferrari S, Frei J, Hofmann F, Mestan J, Mett H, O'Reilly T, Persohn E, Rösel J, Schnell C, Stover D, Theuer A, Towbin H, Wenger F, Woods-Cook K, Menrad A, Siemeister G, Schirner M, Thierauch KH, Schneider MR, Drevs J, Martiny-Baron G, Totzke F. PTK787/ZK 222584, a novel and potent inhibitor of vascular endothelial growth factor receptor tyrosine kinases, impairs vascular endothelial growth factor-induced responses and tumor growth after oral administration. Cancer Res 2000;60:2178–2189.
11. Lee SH, Lopes De Menezes D, Vora J, Harris A, Ye H, Nordahl L, Garrett E, Samara E, Aukerman SL, Gelb AB, Heise C. In vivo target modulation and biological activity of CHIR-258, a multitargeted growth factor receptor kinase inhibitor, in colon cancer models. Clin Cancer Res 2005;11:3633–3641.
12. Kuzniewski CN, Gertsch J, Wartmann M, Altmann KH. Total synthesis of hypermodified epothilone analogs with potent in vitro antitumor activity. Org Lett 2008;10: 1183–1186.
13. Adams J. The development of proteasome inhibitors as anticancer drugs. Cancer Cell 2004;5:417–421.
14. Swift S, Lorens J, Achacoso P, Nolan GP. Rapid production of retroviruses for efficient gene delivery to mammalian cells using 293T cell-based systems. Curr Protoc Immunol 2001; Unit 10:17C.
15. Lorens JB, Bennett MK, Pearsall DM, Throndset WR, Rossi AB, Armstrong RJ, Fox BP, Chan EH, Luo Y, Masuda E, Ferrick DA, Anderson DC, Payan DG, Nolan GP. Retroviral delivery of peptide modulators of cellular functions. Mol Ther 2000;1 (Part 1):438–447.
16. Shaner NC, Campbell RE, Steinbach PA, Giepmans BN, Palmer AE, Tsien RY. Improved monomeric red, orange and yellow fluorescent proteins derived from Discosoma sp. red fluorescent protein. Nat Biotechnol 2004;22:1567–1572.
17. Pettit GR, Singh SB, Hamel E, Lin CM, Alberts DS, Garcia-Kendall D. Isolation and structure of the strong cell growth and tubulin inhibitor combretastatin A-4. Experientia 1989;45:209–211.
18. Dark GG, Hill SA, Prise VE, Tozer GM, Pettit GR, Chaplin DJ. Combretastatin A-4, an agent that displays potent and selective toxicity toward tumor vasculature. Cancer Res 1997;57:1829–1834.
19. Chaplin DJ, Pettit GR, Parkins CS, Hill SA. Antivascular approaches to solid tumour therapy: Evaluation of tubulin binding agents. Br J Cancer Suppl 1996;27: S86–S88.
20. Zanella F, Rosado A, Blanco F, Henderson BR, Carnero A, Link W. An HTS approach to screen for antagonists of the nuclear export machinery using high content cell-based assays. Assay Drug Dev Technol 2007;5:333–341.
21. Rai SS, Wolff J. Localization of the vinblastine-binding site on beta-tubulin. J Biol Chem 1996;271:14707–14711.
22. Ribatti D, Guidolin D, Conconi MT, Nico B, Baiguera S, Parnigotto PP, Vacca A, Nussdorfer GG. Vinblastine inhibits the angiogenic response induced by adrenomedullin in vitro and in vivo. Oncogene 2003;22:6458–6461.
23. Fujita K, Sano D, Kimura M, Yamashita Y, Kawakami M, Ishiguro Y, Nishimura G, Matsuda H, Tsukuda M. Anti-tumor effects of bevacizumab in combination with paclitaxel on head and neck squamous cell carcinoma. Oncol Rep 2007;18: 47–51.
24. Kimura N, Mikami K, Nakamura N, Endoh H. Alteration of developmental program in Paramecium by treatment with trichostatin a: A possible involvement of histone modification. Protist 2006;157:303–314.
25. Rossig L, Li H, Fisslthaler B, Urbich C, Fleming I, Forstermann U, Zeiher AM, Dimmeler S. Inhibitors of histone deacetylation downregulate the expression of endothelial nitric oxide synthase and compromise endothelial cell function in vasorelaxation and angiogenesis. Circ Res 2002;91:837–844.
26. Kim MS, Kwon HJ, Lee YM, Baek JH, Jang JE, Lee SW, Moon EJ, Kim HS, Lee SK, Chung HY, Kim CW, Kim KY. Histone deacetylases induce angiogenesis by negative regulation of tumor suppressor genes. Nat Med 2001;7:437–443.
27. Deroanne CF, Bonjean K, Servotte S, Devy L, Colige A, Clausse N, Blacher S, Verdin E, Foidart JM, Nusgens BV, Castronovo V. Histone deacetylases inhibitors as anti-angiogenic agents altering vascular endothelial growth factor signaling. Oncogene 2002;21:427–436.
28. Shukla N, Freeman N, Gadsdon P, Angelini GD, Jeremy JY. Thapsigargin inhibits angiogenesis in the rat isolated aorta: Studies on the role of intracellular calcium pools. Cardiovasc Res 2001;49:681–689.
29. Takadera T, Ohyashiki T. Calmodulin inhibitor-induced apoptosis was prevented by glycogen synthase kinase-3 inhibitors in PC12 cells. Cell Mol Neurobiol 2007;27:783–790.
30. Sui Y, Wu Z. Alternative statistical parameter for high-throughput screening assay quality assessment. J Biomol Screen 2007;12:229–234.
31. Korff T, Kimmina S, Martiny-Baron G, Augustin HG. Blood vessel maturation in a 3-dimensional spheroidal co-culture model: Direct contact with smooth muscle cells regulates endothelial cell quiescence and abrogates VEGF responsiveness. FASEB J 2001;15:447–457.
32. Dhamodharan R, Jordan MA, Thrower D, Wilson L, Wadsworth P. Vinblastine suppresses dynamics of individual microtubules in living interphase cells. Mol Biol Cell 1995;6:1215–1229.
33. Grigoriev IS, Chernobelskaya AA, Vorobjev IA. Nocodazole, vinblastine and taxol at low concentrations affect fibroblast locomotion and saltatory movements of organelles. Membr Cell Biol 1999;13:23–48.
34. Wang J, Lou P, Lesniewski R, Henkin J. Paclitaxel at ultra low concentrations inhibits angiogenesis without affecting cellular microtubule assembly. Anticancer Drugs 2003; 14:13–19.
35. Heydarkhan-Hagvall S, Helenius G, Johansson BR, Li JY, Mattsson E, Risberg B. Co-culture of endothelial cells and smooth muscle cells affects gene expression of angiogenic factors. J Cell Biochem 2003;89:1250–1259.
36. Kohn EC, Alessandro R, Spoonster J, Wersto RP, Liotta LA. Angiogenesis: Role of calcium-mediated signal transduction. Proc Natl Acad Sci USA 1995;92:1307–1311.
37. Shukla N, Jeremy JY, Nicholl P, Krijgsman B, Stansby G, Hamilton G. Short-term exposure to low concentrations of thapsigargin inhibits replication of cultured human vascular smooth muscle cells. Br J Surg 1997;84:325–330.
38. Birkett SD, Jeremy JY, Watts SM, Shukla N, Angelini GD, Mcardle CA. Inhibition of intracellular Ca2+ mobilisation by low antiproliferative concentrations of thapsigargin in human vascular smooth-muscle cells. J Cardiovasc Pharmacol 1999;33:204–211.